

CRYSTAL GROWTH OF AgSbS₂ (MIARGYRITE) NANOSTRUCTURE BY CYCLIC MICROWAVE RADIATION

J. KAVINCHAN^{a*}, S. THONGTEM^b, E. SAKSORNCHAI^a, T. THONGTEM^{c,d,*}

^a*Division of Chemistry, School of Science, University of Phayao, Phayao 56000, Thailand*

^b*Department of Physics and Materials Science, Faculty of Science, Chiang Mai University, Chiang Mai 50200, Thailand*

^c*Department of Chemistry, Faculty of Science, Chiang Mai University, Chiang Mai 50200, Thailand*

^d*Materials Science Research Center, Faculty of Science, Chiang Mai University, Chiang Mai 50200, Thailand*

Single-crystal growth of silver antimony sulfide (AgSbS₂) nanostructure was successfully synthesized using AgNO₃, Sb(CH₃CO₂)₃ and Na₂S₂O₃·5H₂O dissolved in propylene glycol under a cyclic microwave radiation without the use of any template at 600 W. Phase morphology and vibration mode of the as-synthesized product were characterized by X-ray diffraction (XRD), Fourier transform infrared spectroscopy (FTIR), scanning electron microscopy (SEM) and transmission electron microscopy (TEM). In this research, AgSbS₂ single-crystalline nanostructure was detected. Calculated direct energy gap of AgSbS₂ is 1.75 eV, determined by UV-visible absorption.

(Received May 6, 2015; Accepted June 20, 2015)

Keywords: Cyclic microwave; X-ray diffraction; Electron microscopy

1. Introduction

In recent years, the ternary chalcogenide compounds such as silver antimony sulfide (AgSbS₂) have been very attractive due to their potential applications. Solar cells [1], semiconductor sensitizers [2], micromechanical and optical devices are the samples of different applications [4-8]. The various procedures were used for preparing AgSbS₂ products. For example, a two-stage: ionic layer adsorption and reaction process were used to produce the double-layered structure of AgSbS₂ nanoparticles [2], AgSbS₂ bulks were prepared by a well-established melt quench technique in an electric rocking furnace [3] and microwave-assisted refluxing method was used to synthesize nanostructure flower of nanorods [4].

In this research, cyclic microwave radiation was selected to synthesize AgSbS₂, due to its different benefits such as very simple, fast, inexpensive and extremely effective. This procedure can solve the problems of concentration and temperature gradients. Structure and morphology of products formed under different conditions were characterized by X-ray diffraction (XRD), scanning electron microscopy (SEM) and transmission electron microscopy (TEM). Elemental analysis was studied by energy dispersive X-ray (EDX) detector. The vibration modes were characterized by a Fourier transform infrared spectrometer (FTIR). The direct energy gap was determined by UV-visible absorption. Moreover, the effect of cetyltrimethylammonium bromide (CTAB) addition was also studied.

*Corresponding author: ttphongtem@yahoo.com

2. Experiment

A mixture of 1:1:2 molar ratio of Ag:Sb:S was used to prepare products, 3 mmol of silver nitrate (AgNO_3), 3 mmol of antimony acetate ($\text{Sb}(\text{CH}_3\text{CO}_2)_3$) and 6 mmol of different sulfur sources (sodium thiosulphate ($\text{Na}_2\text{S}_2\text{O}_3 \cdot 5\text{H}_2\text{O}$) and thioacetamide ($\text{C}_2\text{H}_5\text{NS}$)) were dissolved in 30 ml of different solvents (propylene glycol and ethylene glycol) and followed by 15 min stirring. Then, the mixed solutions were irradiated by 300 W, 450 W and 600 W of cyclic microwave radiation for 30 cycles. At the conclusion of the process, black precipitates were synthesized, separated by filtration, washed with deionized water and ethanol, and dried at 70 °C for 24 h.

The as-synthesized phase was characterized by an X-ray diffractometer (XRD, SIEMENS D500) operating at 20 kV 15 mA with K_α line of a copper target. The vibration modes were characterized by a Fourier transform infrared spectrometer (Bruker Tensor 27 FTIR). Their morphologies and purities were investigated by a field emission scanning electron microscope (FE-SEM, JEOL JSM-6335F) operating at 35 kV equipped with an energy dispersive X-ray (EDX) analyzer operating at 15 kV; a transmission electron microscope (TEM, JEOL JEM-2010) with a high resolution transmission electron microscope (HRTEM) and selected area electron diffractometer (SAED) operating at 200 kV; and a UV-visible spectrometer (Lambda 25 PerkinElmer) using a UV lamp with the resolution of 1 nm for a study of its optical property.

3. Results and discussion

At 450 W of microwave power, AgNO_3 and $\text{Sb}(\text{CH}_3\text{CO}_2)_3$ were used as starting materials of silver and antimony sources and the XRD results are shown in Fig. 1. Different sulfur sources and solvents were used in various conditions. The result shows that the pure phase of AgSbS_2 (JCPDS file number 17-0456) [9] was produced with no impurity detection for the use of $\text{Na}_2\text{S}_2\text{O}_3 \cdot 5\text{H}_2\text{O}$ as a sulfur source in propylene glycol. For other conditions, $\text{C}_2\text{H}_5\text{NS}$ in ethylene glycol and $\text{Na}_2\text{S}_2\text{O}_3 \cdot 5\text{H}_2\text{O}$ in ethylene glycol were used and the XRD patterns were specified as AgSbS_2 mixed with some impurities. Additional Sb_2S_3 phase (JCPDS file number 06-0474) [9] and AgSbS_3 phase (JCPDS file number 19-1135) [9] were detected.

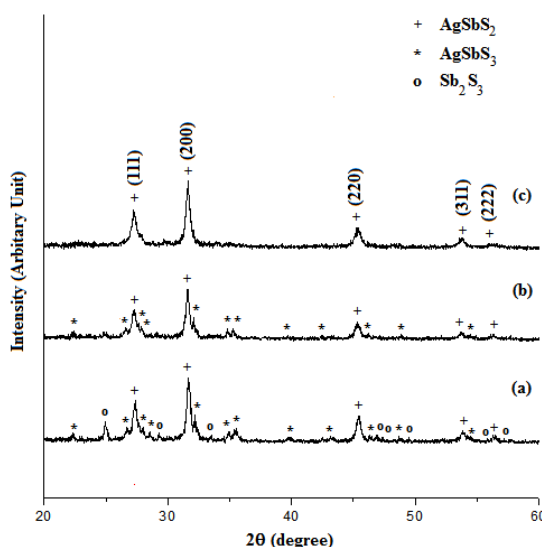


Fig. 1: XRD patterns of products synthesized in the solutions using AgNO_3 and $\text{Sb}(\text{CH}_3\text{CO}_2)_3$ as starting materials with different sulfur sources and solvents of (a) $\text{C}_2\text{H}_5\text{NS}$ in ethylene glycol, (b) $\text{Na}_2\text{S}_2\text{O}_3 \cdot 5\text{H}_2\text{O}$ in ethylene glycol and (c) $\text{Na}_2\text{S}_2\text{O}_3 \cdot 5\text{H}_2\text{O}$ in propylene glycol at 450 W for 30 cycles.

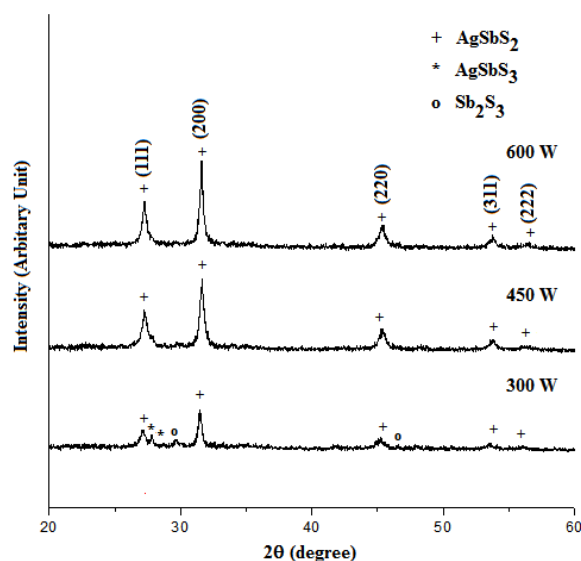


Fig. 2: XRD patterns of products synthesized via cyclic microwave radiation of AgNO_3 , $\text{Sb}(\text{CH}_3\text{CO}_2)_3$ and $\text{Na}_2\text{S}_2\text{O}_3 \cdot 5\text{H}_2\text{O}$ dissolved in propylene glycol at 300 W, 450 W and 600 W microwave powers.

Crystalline phase of AgSbS_2 were obtained by using AgNO_3 , $\text{Sb}(\text{CH}_3\text{CO}_2)_3$ and $\text{Na}_2\text{S}_2\text{O}_3 \cdot 5\text{H}_2\text{O}$ dissolved in propylene glycol at 450 W and 600 W. In contrast, Sb_2S_3 (JCPDS file number 06-0474) [9] and AgSbS_3 (JCPDS file number 19-1135) [9] were also detected at 300 W (Fig. 2). When the microwave power was increased to 450 W and 600 W, the XRD peaks became shaper. These findings imply that the degree of crystallinity of AgSbS_2 phase at 600 W was higher than the AgSbS_2 phase at 450 W. By increasing microwave power, the impurities were also lessened.

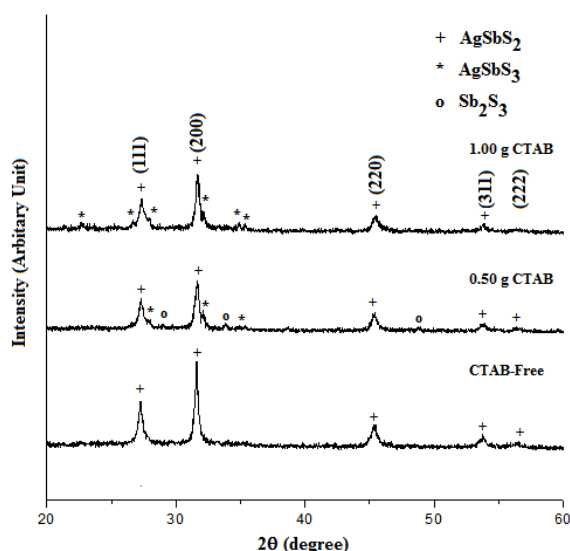


Fig. 3: XRD patterns of products synthesized via cyclic microwave radiation of AgNO_3 , $\text{Sb}(\text{CH}_3\text{CO}_2)_3$ and $\text{Na}_2\text{S}_2\text{O}_3 \cdot 5\text{H}_2\text{O}$ dissolved in propylene glycol at 600 W with and without using CTAB.

The effect of CTAB addition was studied in the solutions of AgNO_3 , $\text{Sb}(\text{CH}_3\text{CO}_2)_3$ and $\text{Na}_2\text{S}_2\text{O}_3 \cdot 5\text{H}_2\text{O}$ dissolved in propylene glycol at 600 W of cyclic microwave radiation (Fig. 3). In the presence of 0.50 g CTAB in the solution, the XRD pattern illustrates that both Sb_2S_3 (JCPDS file number 06-0474) [9] and AgSbS_3 (JCPDS file number 19-1135) [9] phases were also detected.

Only AgSbS_3 phase was detected in the presence of 1.00 g CTAB in the mixed solution. The pH value of each mixed solution was 5. Thus the experimental results show the presence of phase transformation by CTAB-modified nanocrystalline of the obtained products. The AgSbS_2 phase transformed to the mixed phases which were consisted of Sb_2S_3 and AgSbS_3 phases for using 0.50 g of CTAB and only AgSbS_3 phase by using 1.00 g of CTAB. Thus the CTAB is an important agent influencing the phase transformation of the crystal [10].

SEM and TEM images illustrate nanostructure AgSbS_2 synthesized in the solutions with different microwave powers. SEM images (Fig. 4) show AgSbS_2 prepared in the solutions with different microwave powers (300 W, 450 W and 600 W). At 300 W, the obtained precipitates were nanoparticles with different orientations and a wide range of size which were composed of AgSbS_2 , Sb_2S_3 and AgSbS_3 phases. When the microwave power was increased to 450 W, the product was AgSbS_2 incomplete microclusters with different sizes. At 600 W, pure AgSbS_2 microclusters formed which were agglomerated from nanoparticles. The various facets of products were controlled by nucleation, growth procedure and microwave power. Due to the high viscosity of propylene glycol, the crystalline growth was suppressed leading to the formation of agglomerated nanoparticles [11].

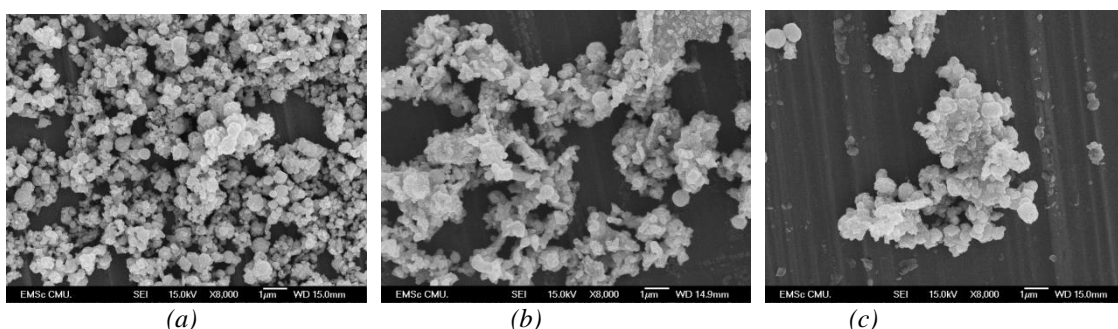


Fig. 4: SEM images of products synthesized via cyclic microwave radiation of AgNO_3 , $\text{Sb}(\text{CH}_3\text{CO}_2)_3$ and $\text{Na}_2\text{S}_2\text{O}_3 \cdot 5\text{H}_2\text{O}$ dissolved in propylene glycol at (a) 300 W, (b) 450 W and (c) 600 W.

TEM and high resolution TEM analysis of these structures indicates that each nanoparticle is single crystal (Fig. 5(a) and 5(b)). The corresponding selected area electron diffraction (SAED) pattern of the product is shown in Fig. 5(c). Obviously, the as-prepared phase is single crystal, and the bright diffraction spots were the indication of its high crystallinity. In addition, the SAED pattern appears as symmetric spots corresponding to the (002), (022) and (020) crystallographic planes of single crystalline cubic AgSbS_2 , in good accordance with the simulated electron diffraction pattern (Fig. 5(d)) [12].

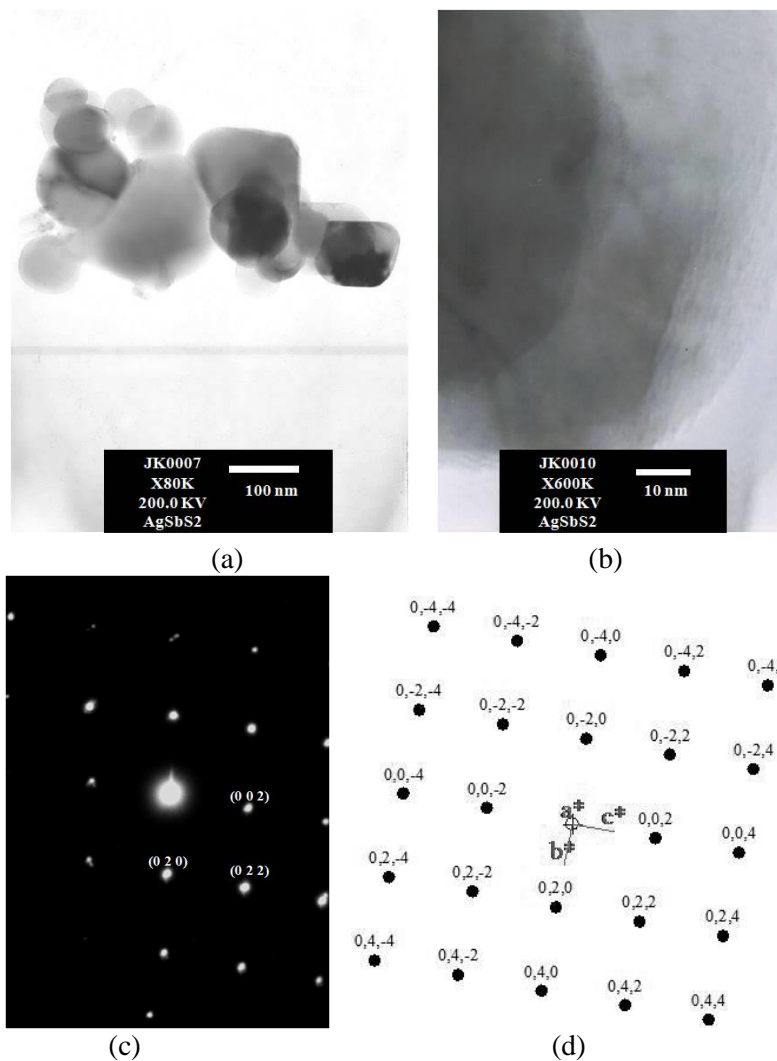


Fig. 5: (a, b) TEM and HRTEM images, and (c, d) SAED and simulated patterns of AgSbS_2 using AgNO_3 , $\text{Sb}(\text{CH}_3\text{CO}_2)_3$ and $\text{Na}_2\text{S}_2\text{O}_3 \cdot 5\text{H}_2\text{O}$ dissolved in propylene glycol synthesized via cyclic microwave radiation at 600 W.

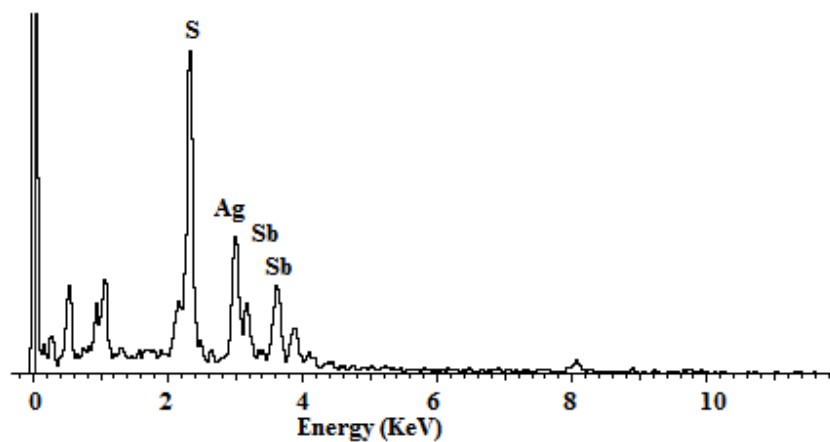


Fig. 6: EDX spectrum of AgSbS_2 synthesized via cyclic microwave radiation at 600 W.

The composition and purity of the as-prepared product were analyzed by EDX analysis (Fig. 6). Quantification of the EDX spectrum provides the atomic ratio of Ag : Sb : S at 1 : 1 : 2,

which was consistent with the stoichiometric composition of AgSbS_2 . No impurities were detected in the EDX spectrum.

Its UV-visible absorption was controlled by two photon energy ($h\nu$) ranges. For $h\nu > E_g$, the curve for direct interband transition was linearly increased with the increasing of photon energy. The allowed direct energy gap was determined by extrapolating linear portion of the curve to zero absorption, and found to be 1.75 eV (Fig. 7) very close to the 1.77-2 eV energy gap of AgSbS_2 reported by Narongrit et al [4] and Ibrahim [5].

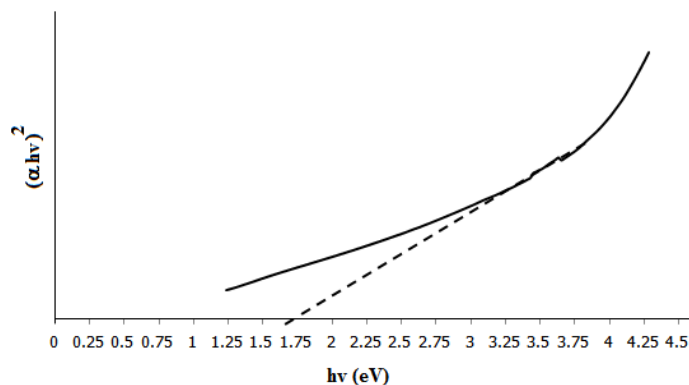


Fig. 7: The $(\alpha h\nu)^2$ vs $h\nu$ plot of AgSbS_2 synthesized via cyclic microwave radiation at 600 W.

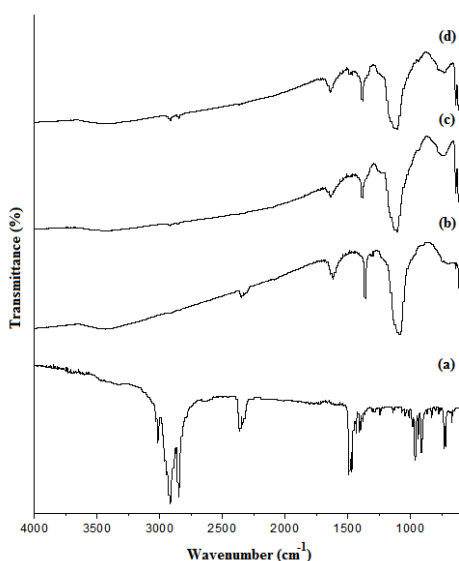


Fig. 8: FTIR spectra of (a) CTAB and the products synthesized via cyclic microwave radiation at 600 W (b) CTAB-free, (c) 0.50 g of CTAB, and (d) 1.00 g of CTAB.

Furthermore, the products were further characterized by FTIR spectroscopy in the range of 400-4000 cm^{-1} and compared to the CTAB powder (Fig. 8). For the CTAB powder, the bands at 3017, 2917 and 2849 cm^{-1} are assigned to the $\nu_{\text{as}}(\text{N-CH}_3)$, $\nu_{\text{as}}(\text{CH}_2)$ and $\nu_{\text{sym}}(\text{CH}_2)$, respectively. The band at 1487 cm^{-1} is attributed to the $\delta_{\text{as}}(\text{N-CH}_3)$ mode. The CH_2 scissoring region at 1462 and 1472 cm^{-1} are related to the $\delta(\text{CH}_2)$ mode. The band at 1396 cm^{-1} is assigned to the $\delta_{\text{sym}}(\text{N-CH}_3)$ and at 912 cm^{-1} to the $\nu(\text{C-N})$. The two bands at 730 and 719 cm^{-1} were specified as the rocking mode of the methylene chain [13-15]. There were no bands corresponding to the CTAB in AgSbS_2 phase without using CTAB powder. In this research, the CTAB was not completely removed by washing with deionized water and ethanol, thus the bands at 2917 and 2849 cm^{-1} were also detected [15].

4. Conclusions

The pure cubic phase of silver antimony sulfide (AgSbS_2) single-crystal nanostructure was successfully synthesized via cyclic microwave radiation at 600 W for 30 cycles of AgNO_3 , $\text{Sb}(\text{CH}_3\text{CO}_2)_3$ and $\text{Na}_2\text{S}_2\text{O}_3 \cdot 5\text{H}_2\text{O}$ in propylene glycol. The phase, morphology and vibration mode were detected by XRD, SEM, TEM and FTIR. SEM and TEM revealed that the as-synthesized product was nanostructure with its calculated allowed direct energy gap of 1.75 eV.

Acknowledgement

We are extremely grateful to the Thailand's Office of the Higher Education Commission for financial support through the National Research University (NRU) Project for Chiang Mai University.

References

- [1] J. G. Garza, S. Shaji, A. C. Rodriguez, T. K. Das Roy, B. Krishnan, *Appl. Surf. Sci.* 257, 10834 (2011).
- [2] Y. R. Ho, M. W. Lee, *Electrochem. Commun.* 26, 48 (2013).
- [3] J. Gutwirth, T. Wágner, E. Kotulánová, P. Bezdička, V. Peřina, M. Hrdlička, M. Vlček, Č. Drašar, M. Frumar, *J. Phys. Chem. Solids* 68, 835 (2007).
- [4] N. Tipcompor, S. Thongtem, T. Thongtem, *J. Nanomater.* 2013, Article 970489, 2013.
- [5] A. M. Ibrahim, *J. Phys.* 7, 5931 (1995).
- [6] T. Wagner, J. Gutwirth, P. Nemeč et al., *Appl. Phys. A* 79, 1561 (2004).
- [7] J. Gutwirth, T. Wágner, P. Němec, S. O. Kasap, M. Frumar, *J. Non-Crystal. Solids* 354, 497 (2008).
- [8] S. Berri, D. Maouche, N. Bouarissa and Y. Medkour, *Mater. Sci. Semicond. Proc.* 16, 1439 (2013).
- [9] Powder Diffract. File, JCPDS-ICDD, 12 Campus Boulevard, Newtown Square, PA 19073-3273, USA, 2001.
- [10] R.B. Viana, A. B. F. da Silva, A. S. Pimentel, *Adv. Phys. Chem.* 2012, Article 903272, (2012).
- [11] S. Kaowphong, T. Thongtem, O. Yayapao and S. Thongtem, *Mater. Lett.* 65, 3405 (2011).
- [12] C. Boudias, D. Monceau, "CaRIne Crystallography 3. 1, DIVERGENT S.A.," Centre de Transfert, Compiègne, France, 1989–1998.
- [13] Z. M. Sui, X. Chena, L.Y. Wang, L.M. Xu, W.C. Zhuang, Y.C. Chai, C.J. Yang, *Physica E*, 33, 308 (2006).
- [14] Y. Qu, W. Wang, L. Jing, S. Song, X. Shi, L. Xue, H. Fu, *Appl. Surf. Sci.* 257, 151 (2010).
- [15] O. Yayapaoa, T. Thongtema, A. Phuruangrat, S. Thongtem, *J. Alloys Compd.* 509, 2294 (2011).